International Journal of Pharmaceutics 420 (2011) 191–197

Contents lists available at SciVerse ScienceDirect

International Journal of Pharmaceutics

journal homepage: www.elsevier.com/locate/ijpharm

Guest molecular size-dependent inclusion complexation of parabens with cholic acid by cogrinding

Kunikazu Moribe[a], Miyuki Masaki[a], Ryo Kinoshita[a], Junying Zhang[a], Waree Limwikrant[a], Kenjirou Higashi[a], Yuichi Tozuka[b], Toshio Oguchi[c], Keiji Yamamoto[a,*]

[a] Graduate School of Pharmaceutical Sciences, Chiba University, 1-8-1 Inohana, Chuo-ku, Chiba 260-8675, Japan
[b] Gifu Pharmaceutical University, 5-6-1 Mitahora-higashi, Gifu 502-8585, Japan
[c] Department of Pharmacy, University of Yamanashi, 1110 Shimogato, Chuo City 409-3898, Japan

ARTICLE INFO

Article history:
Received 3 June 2011
Received in revised form 2 August 2011
Accepted 16 August 2011
Available online 22 August 2011

Keywords:
Cholic acid
Paraben
Inclusion complex
Crystal structure
Solid-state NMR
Cogrinding

ABSTRACT

Effects of *p*-hydroxybenzoate (paraben) ester chain length on the stoichiometry and structure of grinding-induced inclusion complexes with cholic acid (CA) were investigated. Physicochemical properties of the ground mixture were evaluated by powder X-ray diffraction (PXRD), differential scanning calorimetry (DSC), Fourier transform infrared (FT-IR) spectroscopy, and solid-state nuclear magnetic resonance (NMR) measurements. Ethyl-, *n*-propyl-, and isopropyl-parabens formed equimolar inclusion complexes with CA, and the complex structures were of the *β-trans* bilayer type. In contrast, the stoichiometry of the CA–paraben complex was 2:1, and the structure was of the *α-gauche* bilayer type when isobutylparaben was used as a guest molecule. Although the stoichiometries and structures of the complexes differed, solid-state NMR showed that the molecular states of parabens in the complexes were similar and independent of the ester chain length. Complexes between CA and parabens with longer substituent groups (C >4) were not observed. Steric effects induced by increasing the guest size are likely to influence the overall structure of inclusion complexes. Mechanical forces and thermal activation by grinding were important factors in the mechanism of CA–paraben complex formation.

1. Introduction

In humans, the most important bile acids are cholic acid (CA), deoxycholic acid (DCA), and chenodeoxycholic acid. Bile acids play an important role in the absorption of lipids by micellar formation. DCA can provide tunnel-like spaces called channels, in which a wide variety of organic molecules can be accommodated during complex formation (Miki et al., 1990). The channel size can be adjusted depending on the size of the guest molecules, resulting in effective complexation with many compounds (Oguchi et al., 2000). The structure of CA includes an additional hydroxyl group compared to DCA (Fig. 1). It has a facially amphiphilic molecular structure, i.e., three hydroxyl groups directed toward the steroid α-face to form a hydrophilic face and two methyl groups turned toward another face (β-face) to form a lipophilic face (Nakano et al., 2005). CA generally forms two types of host frameworks when complexed with guest molecules (Sada et al., 2001). One is a crossing-type or non-channel structure, which was reported in the case of small guest molecules such as methanol, ethanol, and 1-propanol (Johnson and Schaefer, 1972; Jones and Nassimbeni, 1990). The other is a bilayer-type or channel structure providing channels or void spaces in which larger guest molecules can be accommodated, e.g., acetophenone (Miki et al., 1988) and methyl *p*-hydroxybenzoate (Oguchi et al., 2002). In bilayer structures, the host frameworks were classified into four subtypes based on conformational isomerization of the steroidal side chain (*gauche* and *trans*) and stacking modes of the methyl groups in the lipophilic layer (α and β) (Nakano et al., 2001). There were *α-gauche*, *α-trans*, *β-gauche*, and *β-trans* types, which had identical host–host hydrogen-bond networks, and the lipophilic host channels with slightly different steric dimension. Bohne et al. have reported on how the hydrophobic and hydrophilic compounds can be mixed with the bile acids, such as sodium cholate in aqueous solution (Yihwa et al., 2004; Waissbluth et al., 2006).

The conventional method used to prepare complexes of bile acids is coprecipitation. However, some solvents can be preferentially included in the cavity instead of the guest compound. Cogrinding is an alternative method for preparing inclusion complexes such as DCA–naphthalene, CA–ibuprofen, and ursodeoxycholic acid–phenanthrene (Oguchi et al., 1998, 2002, 2003). Molecular complexation between bile acids and guest compounds has been explored since the 1990s. For example, the effect of guest species on the complex formation of DCA by cogrinding has been reported (Oguchi et al., 1998). In this study, parabens were used as guest molecules. Parabens are often used in the

* Corresponding author. Tel.: +81 43 226 2865; fax: +81 43 226 2867.
E-mail address: k-yamamoto@faculty.chiba-u.jp (K. Yamamoto).

0378-5173/$ – see front matter © 2011 Elsevier B.V. All rights reserved.
doi:10.1016/j.ijpharm.2011.08.027

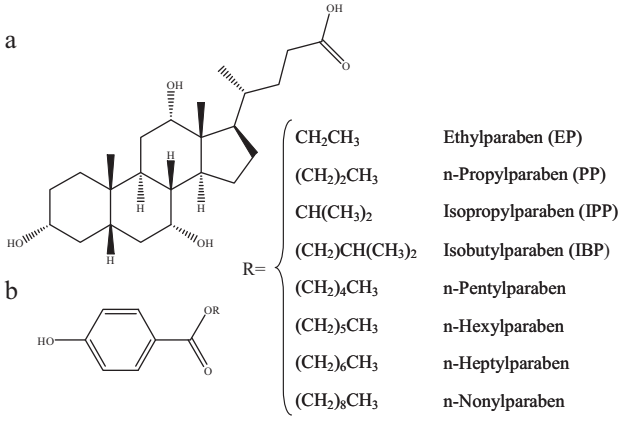

Fig. 1. Chemical structures of (a) CA and (b) parabens.

pharmaceutical formulations as preservatives. Complex formation between a paraben and the other compositions in the formulation could affect the preservation property. We investigated the grinding-induced inclusion complexes between CA and parabens with different substitute groups and examined the molecular state of the guest molecules in these complexes. We discussed mechanisms of CA–isopropylparaben and CA–isobutylparaben complex formation.

2. Materials and methods

2.1. Materials

CA (purity 98%) was purchased from Nacalai Tesque, Inc. (Japan). Parabens used in this study were ethylparaben (EP), *n*-propylparaben (PP), isopropylparaben (IPP), isobutylparaben (IBP), *n*-pentylparaben, *n*-hexylparaben, *n*-heptylparaben, and *n*-nonylparaben. Their chemical structures are shown in Fig. 1. All parabens were obtained from Tokyo Chemical Industry Co., Ltd. (Japan) and were of reagent grade with a purity of >99%.

2.2. Preparation of CA–paraben physical mixtures (PMs) and ground mixtures (GMs)

CA–paraben PMs were prepared at various molar ratios using a vortex mixer by mixing for 5 min. Each PM (3 g) was loaded in a mill chamber made of aluminum oxide and ground using a CMT TI-200 vibrational mill (CMT Co., Ltd., Japan) for 60 min to obtain GMs (except CA–IBP GM). To avoid melting of IBP during cogrinding, CA–IBP GM was prepared by grinding the PM for 90 min with pauses every 30 min of milling. For low-temperature grinding (−180 °C), the PM was loaded in a stainless steel chamber and ground using a CMT TI-500 vibration rod mill (CMT Co., Ltd., Japan). Liquid nitrogen was fed gradually until the temperature dropped to −180 °C before grinding.

2.3. Preparation of CA–paraben sealed-heating samples (SHs)

The PM of CA and paraben (200 mg) was placed in a 2.0-mL glass ampoule. The ampoule was sealed, heated to 40 °C for CA–IPP and 60 °C for CA–IBP and kept isothermally for 2 h.

2.4. Powder X-ray diffraction (PXRD) measurements

X-ray diffractograms were obtained using a Rigaku Miniflex powder X-ray diffractometer (Rigaku Corporation, Japan). The measurement conditions were as follows: target, Cu; filter, Ni; voltage 30 kV; current 15 mA; and scanning speed 4°/min over a 2θ range of 5–35°.

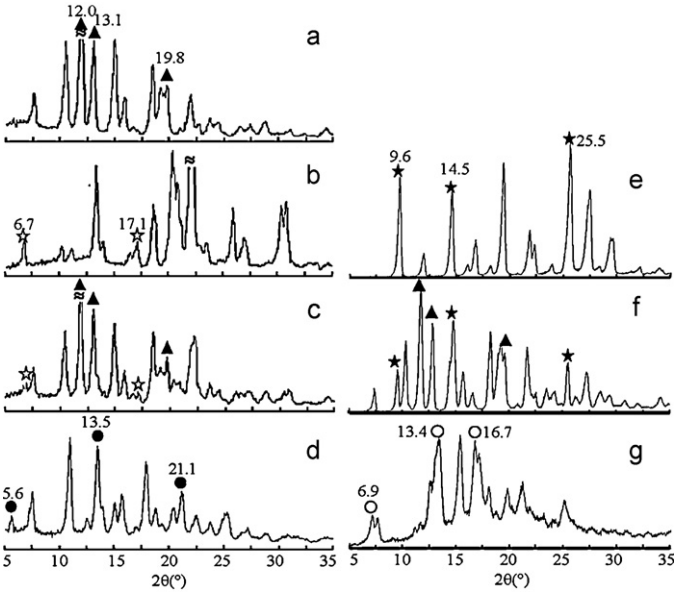

Fig. 2. Changes in the PXRD patterns of the 1:1 CA–IPP and 2:1 CA–IBP systems after cogrinding. (a) CA, (b) IPP, (c) physical mixture of CA–IPP, (d) ground mixture of CA–IPP, (e) IBP, (f) physical mixture of CA–IBP, and (g) ground mixture of CA–IBP (▲: CA; ☆: IPP; ●: CA–IPP complex; ★: IBP; ○: CA–IBP complex).

2.5. Differential scanning calorimetry (DSC)

DSC measurements were performed using a DSC-3100 (Mac Science, Japan) and EXSTAR6000 DSC6200 (SII Nano Technology, Japan) for CA–IPP and CA–IBP systems, respectively. Each sample (ca. 3 mg) was measured in an aluminum open-pan system under a constant purge of nitrogen over a temperature range of 50–230 °C at a heating rate of 5 °C/min. Prior to DSC analysis, the system was calibrated using indium as a reference standard.

2.6. Fourier transform infrared (FT-IR) spectroscopy

FT-IR spectra were obtained by the KBr method with an FT-IR 230 spectrometer (JASCO Corporation, Japan) and ALPHA FT-IR spectrometer (Bruker Optics Corporation, Japan) for CA–IPP and CA–IBP systems, respectively. All spectra represent 32 averaged scans at a resolution of 4.0 cm^{-1}.

2.7. Solid-state nuclear magnetic resonance (NMR) spectroscopy

All ^{13}C solid-state NMR spectra were recorded using a JNM-ECX 400 NMR spectrometer (JEOL Ltd., Japan). Powder samples were placed into 6-mm zirconia rotors. All spectra were acquired using a sequence of variable-amplitude cross-polarization (CP), total spinning sideband suppression, and a high-power two-pulse phase-modulation ^1H decoupling. The magic angle spinning (MAS) was applied at a rotational speed of 6 kHz. The total scan for each sample (1000–14,400) depended on the signal-to-noise ratio required. Pertinent acquisition parameters included a CP contact time of 2 ms, a ^1H 90° pulse of 5.5 μs, and relaxation delays of 3 s. A total of 4096 data points were acquired for each experiment. All spectra were externally referenced by setting the methine peak of hexamethylbenzene to 17.3 ppm.

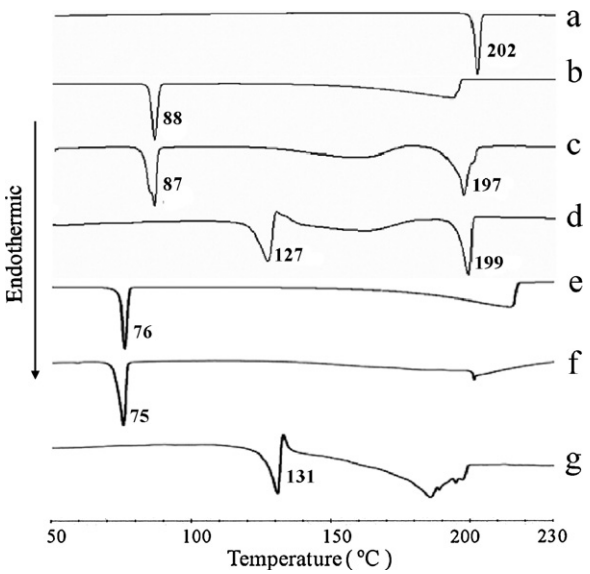

Fig. 3. DSC curves of the 1:1 CA–IPP and 2:1 CA–IBP systems. (a) CA, (b) IPP, (c) physical mixture of CA–IPP, (d) ground mixture of CA–IPP, (e) IBP, (f) physical mixture of CA–IBP, and (g) ground mixture of CA–IBP.

3. Results and discussion

3.1. Cogrinding of CA and parabens

Effects of paraben ester chain length on inclusion complex formation with CA were investigated. We used several paraben derivatives, as mentioned in Section 2.1. The guest compounds IPP and IBP are discussed.

Fig. 2a–d shows the PXRD patterns of the CA–IPP system at a molar ratio of 1:1. Characteristic peaks were observed at $2\theta = 12.0^\circ$, 13.1°, and 19.8° for CA (Fig. 2a) and 6.7° and 17.1° for IPP (Fig. 2b). The PXRD pattern of the PM was the superimposition of the diffraction peaks of CA and IPP crystals (Fig. 2c). When the PM was ground for 60 min, the peaks in the PM disappeared, and new peaks were observed at 5.6°, 13.5°, and 21.1° (Fig. 2d). After grinding each component individually for 60 min, the diffraction pattern of CA exhibited a halo pattern, while that of IPP showed no change (data not shown). This result suggested that a new equimolar crystalline complex was formed between CA and IPP by cogrinding. Subsequently, the host framework of the complex was determined by comparison with the known inclusion complexes of CA. The CA–IPP complex had a diffraction pattern similar to those of inclusion complexes of CA with ethylbenzene, allylbenzene, and benzyl chloride (Nakano et al., 2001; Supplementary Fig. 1S). Those structures have

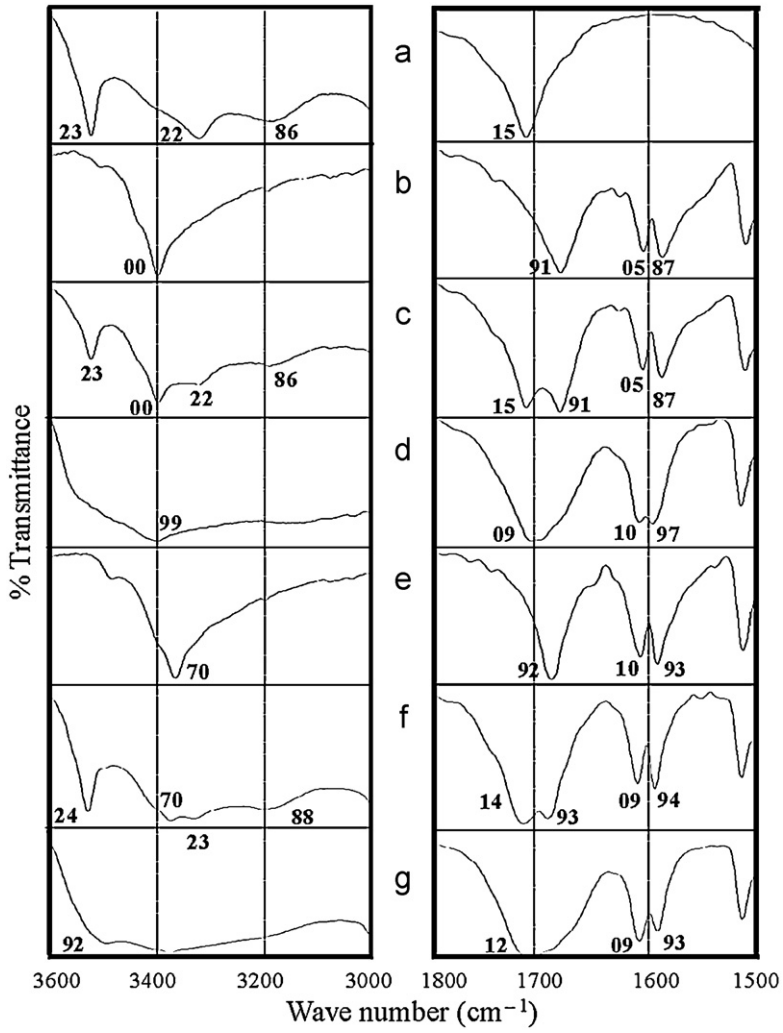

Fig. 4. FT-IR spectra of the 1:1 CA–IPP and 2:1 CA–IBP systems. (a) CA, (b) IPP, (c) physical mixture of CA–IPP, (d) ground mixture of CA–IPP, (e) IBP, (f) physical mixture of CA–IBP, and (g) ground mixture of CA–IBP.

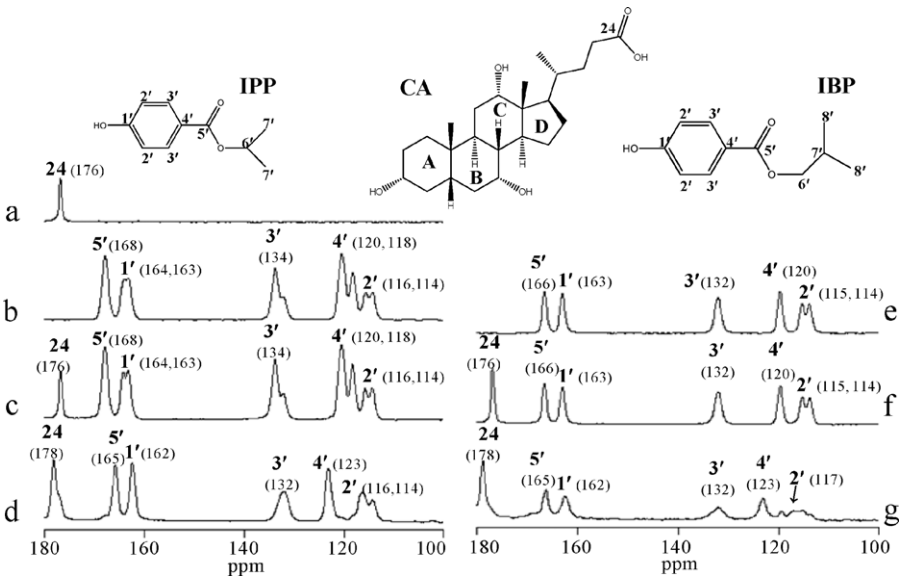

Fig. 5. ^{13}C-CP/MAS NMR spectra of the 1:1 CA–IPP and 2:1 CA–IBP systems. (a) CA, (b) IPP, (c) physical mixture of CA–IPP, (d) ground mixture of CA–IPP, (e) IBP, (f) physical mixture of CA–IBP, and (g) ground mixture of CA–IBP.

been reported as *β-trans* bilayer type. Therefore, the CA–IPP complex presumably had a *β-trans* bilayer-type structure.

Fig. 3a–d shows DSC measurements of the CA–IPP system. CA and IPP crystals showed endothermic peaks due to fusion at 202 and 88 °C, respectively. The DSC curve of the PM had two fusion peaks derived from CA and IPP crystals at 197 and 87 °C, respectively. For the GM, the endothermic peak, presumably corresponding to fusion of the complex, was observed at 127 °C, indicating complex formation between CA and IPP by cogrinding. After melting the complex, CA recrystallization followed by fusion at 199 °C was observed.

Molecular interactions between CA and IPP in the grinding-induced complex were investigated using FT-IR spectroscopy in Fig. 4a–d. The CA crystal showed O–H stretching bands at 3523, 3322, and 3186 cm^{-1} and a carbonyl stretching peak at 1715 cm^{-1} (Fig. 4a). The IR spectrum of IPP (Fig. 4b) had an O–H stretching peak at 3400 cm^{-1}, carbonyl stretching peak at 1691 cm^{-1}, and C=C stretching bands of the benzene ring at 1605 and 1587 cm^{-1}. The PM spectrum (Fig. 4c) was the superimposition of the spectral patterns of CA and IPP crystals. Remarkable changes were observed in the GM spectrum: a new peak at 1709 cm^{-1} and broadening of the O–H stretching peak (Fig. 4d). The crystal structure of CA without a guest molecule did not contain channels (Miki et al., 1990). When CA formed a complex with guest molecules, the carbonyl group of CA molecules formed hydrogen bonds with OH groups of neighboring CA molecules to provide channels for the guest compound in the structure of the CA–guest complex (Nakano et al., 1994). Therefore, the changes observed in the GM IR spectrum indicated the formation of a channel structure in which IPP was accommodated, and the molecular arrangements of CA and IPP in GM differed from those in PM. In addition, C=C stretching of the benzene ring in IPP shifted from 1587 cm^{-1} to 1597 cm^{-1}. This shift can be explained by van der Waals interactions of CA and IPP molecules, as observed in other bile acid complexes (Limmatvapirat et al., 1997; Oguchi et al., 2002). From these results, it can be concluded that cogrinding induced the formation of an equimolar CA–IPP inclusion complex.

Molecular states of IPP guest molecules in the inclusion complex were investigated by solid-state NMR spectroscopy. The ^{13}C-CP/MAS spectra of the CA–IPP system are presented in Fig. 5a–d. Since the paraben chain length showed chemical shifts at high magnetic fields, which overlapped with the chemical shift of most CA carbon atoms, comparison between the NMR spectra of the PM and GM was performed in the range of 100–180 ppm. Peaks of carbon atoms at position 24 of CA and at positions 1′, 3′, 4′, and 5′ of IPP shifted, revealing that the chemical environment of neighboring molecules changed, and this may have resulted from new intermolecular interactions (Kuo and Chang, 2001; Vogt et al., 2009). The results suggested that the molecular state of IPP in the GM was different from that in the PM, reflecting the interaction of IPP with CA due to inclusion complex formation.

IBP, a paraben with a butyl group at the side chain, was used to investigate the formation of inclusion complexes with CA. Fig. 2e–g shows the PXRD patterns of the CA–IBP system. Diffraction peaks of IBP crystals were observed at $2\theta = 9.6°$, 14.5°, and 25.5° (Fig. 2e). After grinding the PM at a molar ratio of 1:1, new PXRD peaks were observed at 6.9°, 13.4°, and 16.7°, corresponding to a new complex and the remaining peak of IBP. When the molar ratio of CA:IBP was changed to 2:1, new diffraction peaks were observed with no peak corresponding to the starting materials (Fig. 2g). The diffraction pattern of the GM was completely different from that of

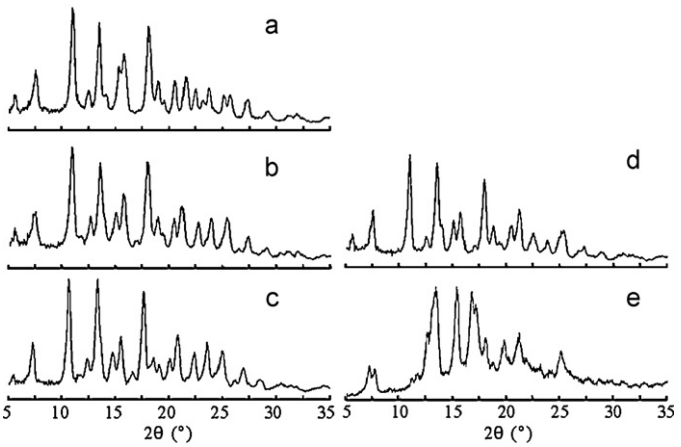

Fig. 6. PXRD patterns of various CA–paraben complexes prepared by cogrinding. (a) 1:1 CA:methyl paraben, (b) 1:1 CA:EP, (c) 1:1 CA:PP, (d) 1:1 CA:IPP, and (e) 2:1 CA:IBP. Parabens with longer substituent groups (*n*-pentylparaben, *n*-hexylparaben, *n*-heptylparaben, and *n*-nonylparaben) did not form complexes with CA by cogrinding.

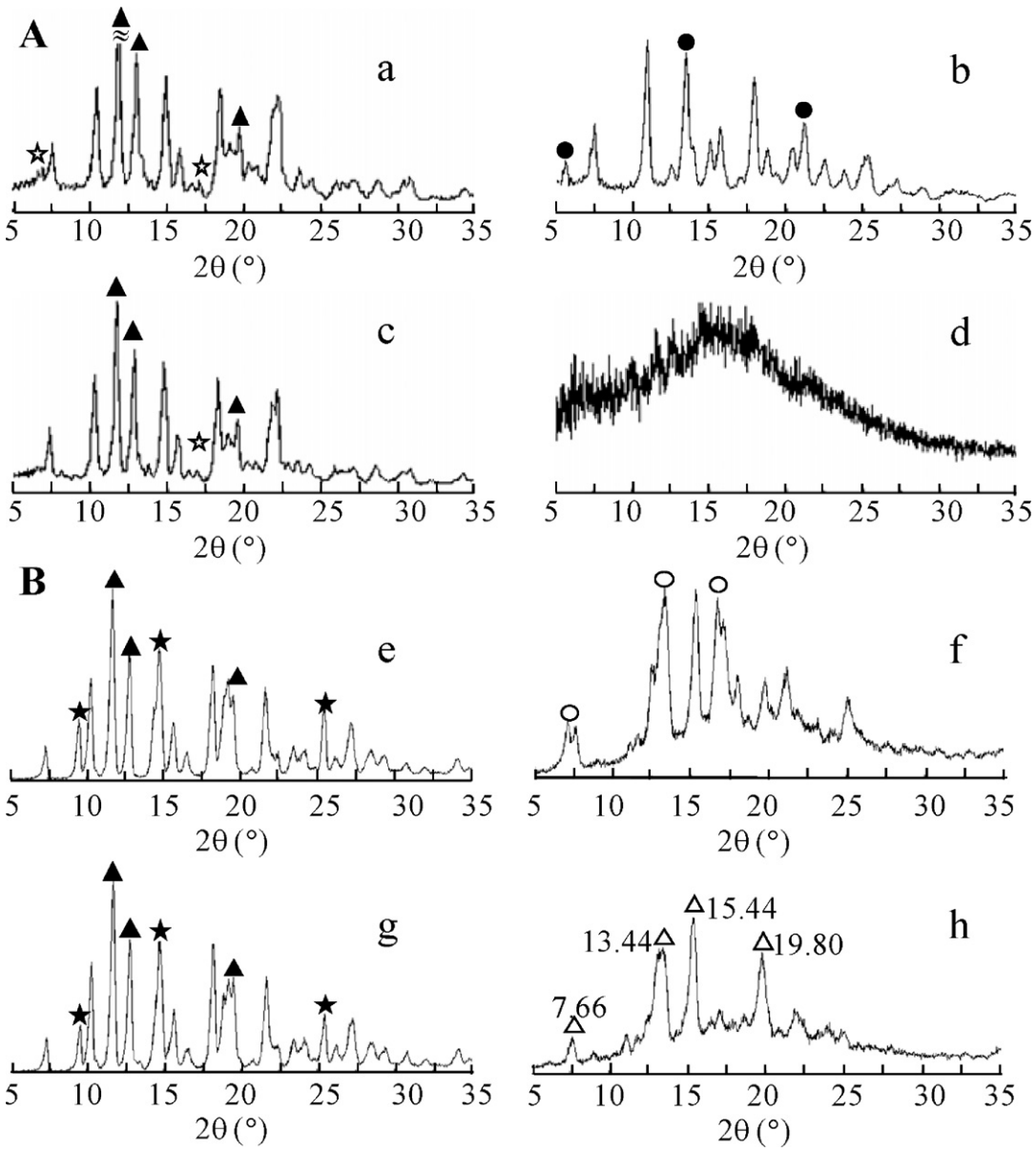

Fig. 7. PXRD patterns of (A) the 1:1 CA–IPP and (B) the 2:1 CA–IBP systems after low-temperature grinding (−180 °C) and sealed-heating process. Physical mixture of 1:1 CA–IPP, (b) ground mixture of 1:1 CA–IPP, (c) sample (a) after sealed-heating at 40 °C for 2 h, (d) sample (a) after grinding at −180 °C for 60 min, (e) physical mixture of 2:1 CA–IBP, (f) ground mixture of 2:1 CA–IBP, (g) sample (e) after sealed-heating at 60 °C for 2 h, and (h) sample (e) after grinding at −180 °C for 90 min and then sealed-heating at 60 °C for 2 h (▲: CA; ☆: IPP; ●: CA–IPP complex; ★: IBP; ○: CA–IBP complex; △: cholic acid hemihydrate).

2:1 PM (Fig. 2f). These results indicated that the CA–IBP complex likely formed at a molar ratio of 2:1 by cogrinding. The stoichiometry of CA-monosubstituted benzene inclusion complexes varied depending on the size and shape of the guest compounds (Nakano et al., 2001). For larger guest compounds, the stoichiometry of the host and guest might not be 1:1 because more CA molecules are required to accommodate guest molecules into the channels. This might explain why the stoichiometry of the CA–IBP system (2:1) was higher than that of the CA–IPP system (1:1). The frequently observed inclusion complexes of CA are bilayer-type structures with molar ratios of 1:1 or 2:1 (host:guest). In addition, based on X-ray crystallographic data, the CA–IBP complex was presumed to be an *α-gauche* bilayer-type structure, which has been observed in crystal structures of CA inclusion complexes with toluene, styrene, and fluorobenzene (Nakano et al., 2001; Supplementary Fig. 2S).

Fig. 3e–g shows DSC curves of the CA–IBP system. An endothermic peak due to the fusion of IBP crystals was observed at 76 °C. The DSC curve of the PM at a molar ratio of 2:1 shows the fusion peaks of IBP and CA at 75 and 201 °C, respectively. For the GM at a molar ratio of 2:1, the melting peak of IBP disappeared, and an endothermic peak corresponding to the fusion peak of a new crystalline complex of CA and IBP was observed at 131 °C. This result agreed with the result from PXRD measurements, indicating complex formation between CA and IBP at a molar ratio of 2:1. Fig. 4e–g shows FT-IR spectra of the CA–IBP system. The spectrum of IBP crystals showed O–H stretching at 3370 cm^{-1}, carbonyl stretching at 1692 cm^{-1}, and C=C stretching of the benzene ring at 1610 and 1593 cm^{-1}. For the PM, all observed bands were derived from CA and IBP crystals. In the GM spectrum, a broad band due to hydroxyl groups and changes in carbonyl groups of CA and IBP were observed, indicating that the molecular arrangement of CA and IBP in the PM differed from that in the GM.

Fig. 5e–g shows ^{13}C-CP/MAS spectra of the CA–IBP system. The GM spectrum shows that the chemical shifts of carbon atoms at

position 24 of CA and at positions 1′, 2′, 4′, and 5′ of IBP shifted, indicating that the molecular state of IBP changed due to cogrinding with CA. It is noteworthy that the peak shape and chemical shift of IBP in the CA–IBP GM spectrum (Fig. 5g) were very similar to those of IPP in the CA–IPP GM spectrum (Fig. 5d). The NMR peak shape and chemical shift of the IBP spectrum (Fig. 5e) differed from those of the IPP spectrum (Fig. 5b) due to their crystal packing, although only the chain length was different in their chemical structures. However, when forming inclusion complexes with CA, guest molecules should be accommodated in the CA structure in a similar arrangement, regardless of different stoichiometries and host structures of the complexes.

In addition to IPP and IBP, complexes of CA with other parabens, including EP, PP, BP, *n*-pentylparaben, *n*-hexylparaben, *n*-heptylparaben, and *n*-nonylparaben, were investigated by PXRD. As shown in Fig. 6, EP and PP formed 1:1 crystalline complexes with CA. Based on PXRD patterns, CA–IPP, CA–EP, and CA–PP complexes had identical PXRD patterns to that of the CA–methylparaben complex reported by Oguchi et al. (2002), indicating the similarity of the overall crystal structures. The crystal structures of host frameworks are likely to be a *β-trans* bilayer-type structure. Parabens with longer ester chain lengths (*n*-pentylparaben, *n*-hexylparaben, *n*-heptylparaben, and *n*-nonylparaben) did not form complexes with CA by cogrinding, suggesting that the CA channel was limited by steric hindrance due to increasing size of the guest compound. From these results, it can be concluded that paraben ester chain length plays an important role in CA–paraben complex formation.

3.2. Mechanism of CA–paraben inclusion complex formation

Changes in the PXRD patterns of CA–IPP (1:1) and CA–IBP (2:1) systems by sealed-heating and low-temperature grinding are shown in Fig. 7. Each diffraction pattern of SH samples (Fig. 7c and g) was the same as that observed in the PMs (Fig. 7a and e), indicating that thermal activation alone was not enough to facilitate complexation. Oguchi et al. (2002) reported that a CA–methylparaben inclusion complex could be prepared by the sealed-heating method. This means that thermal activation can induce complex formation. During sealed-heating preparation (115 °C), methylparaben can sublime and interact with the CA crystal. From the material safety data sheets, parabens with longer substituent groups have lower vapor pressures than those with shorter substituent groups, i.e., butylparaben (0.000180 mmHg) < methylparaben (0.006000 mmHg) at 25 °C. In addition, the vapor pressure of IBP is only 0.5 mmHg at 145 °C. In our study, when IPP or IBP was used as the guest molecule, heat treatment (at 40 °C for CA–IPP and 60 °C for CA–IBP) resulted in low vapor pressures, which were insufficient to interact with CA and form new crystalline complexes. On the other hand, when the PM of CA and guest compounds (IPP or IBP) was ground, the complex was formed (Fig. 7b and f). For vibrational rod milling, the temperature of the grinding cell usually increases during grinding. Thus, thermal activation and mechanical force contributed to the formation of a new crystalline complex. To clarify the mechanism, low-temperature grinding was performed at −180 °C. PXRD results for an equimolar CA–IPP system showed a halo pattern for the low-temperature ground sample, and the pattern changed to that observed in the GM after sealed-heating at 40 °C for 2 h. This indicated the formation of an equimolar CA–IPP complex. Thus, mechanical force followed by heat treatment was sufficient to form a complex; simultaneous processing is not necessary to form a CA–IPP complex. In the CA–IBP system, the low-temperature ground sample was also in an amorphous state, suggesting that the crystal structures of the starting materials were disordered. However, the diffraction peaks of the low-temperature ground sample after heat treatment (60 °C, 2 h) were different from that of the GM. Its PXRD pattern had peaks similar to those derived from cholic acid hemihydrate (Lessinger and Low, 1993; Supplementary Fig. 3S). Although the recrystallization of IBP was not observed by PXRD measurements, NMR measurements confirmed the existence of IBP crystal nuclei (Supplementary Fig. 4S). When amorphous ground CA was kept at 40 °C, 82% relative humidity, it became cholic acid hemihydrate. Based on our data, it is probable that the crystallization of cholic acid hemihydrate occurred after heat treatment of the low-temperature ground sample, indicating that no complex formed between CA and IBP when low-temperature grinding and heating were performed separately. It is proposed that mechanical forces that break the crystal structure of the starting materials into an unstable state and thermal activation facilitating the crystallization of new complexes were simultaneously required for complex formation of CA and IBP. It is hard to identify the certain reason why the formation of CA complexes could be formed only by simultaneous process (mechanical force and thermal activation during cogrinding), whereas some could be prepared by separated process. It was speculated that the difference in stoichiometry and structures of CA–IPP and CA–IBP complexes may affect the formation of their complexes. It should be noted that the PXRD pattern of CA–IBP low-temperature ground sample after heat treatment at 40 °C for 2 h was halo pattern. It might need more energy comparing to CA–IPP complex. By taking the grinding time into consideration, a longer grinding time (90 min) was needed to prepare the CA–IBP complex compared to the CA–IPP complex (60 min). These finding implied that higher energy was required to prepare the CA–IBP complex.

4. Conclusions

Channel-type inclusion complexes of CA and parabens were prepared by cogrinding. Ester chain length plays an important role in inclusion complexation. Parabens with different ester chain lengths form different stoichiometric and structural inclusion complexes with CA. EP, PP, and IPP formed inclusion complexes with CA at a molar ratio of CA:paraben = 1:1 with a *β-trans* bilayer-type structure. The 2:1 complex with an *α-gauche* bilayer-type structure was obtained by cogrinding CA with IBP. Although there were differences in the stoichiometries and structures of CA–IPP and CA–IBP complexes, the molecular states of guest molecules (IPP/IBP) in the CA structure were relatively similar based on NMR results. Parabens with longer substituent groups did not form CA inclusion complexes. It is probable that steric effects caused by the increased size of the guest molecules affected the formation of inclusion complexes. The mechanism of CA–IPP and CA–IBP complex formation was related to mechanical forces that break the structure of the starting materials and to thermal activation for crystallization of complex nuclei.

Acknowledgement

This study was supported by a Grant-in-Aid for Scientific Research from the Ministry of Education, Culture, Sports, Science, and Technology (Monbukagakusho), Japan (21790032, 21590038).

Appendix A. Supplementary data

Supplementary data associated with this article can be found, in the online version, at doi:10.1016/j.ijpharm.2011.08.027.

References

Johnson, P.L., Schaefer, J.P., 1972. The crystal and molecular structure of an addition compound of cholic acid and ethanol. Acta Crystallogr. B 28, 3083–3088.

Jones, E.L., Nassimbeni, L.R., 1990. Crystal and molecular structures of the inclusion compounds of cholic acid with methanol, ethanol and 1-propanol. Acta Crystallogr. B 46, 399–405.
Kuo, S.W., Chang, F.C., 2001. Studies of miscibility behavior and hydrogen bonding in blends of poly(vinylphenol) and poly(vinylpyrrolidone). Macromolecules 34, 5224–5228.
Lessinger, L., Low, B.W., 1993. Crystal structure and hydrogen-bonding system of cholic acid hemihydrate, $C_{24}H_{40}O_5 \cdot 1/2H_2O$. J. Chem. Crystallogr. 23, 85–99.
Limmatvapirat, S., Yonemochi, E., Oguchi, T., Yamamoto, K., 1997. Complex formation between deoxycholic acid and menadione by grinding and sealed heating methods. Chem. Pharm. Bull. 45, 1358–1362.
Miki, K., Kasai, N., Shibakami, M., Chirachanchai, S., Takemoto, K., Miyata, M., 1990. Crystal structure of cholic acid with no guest molecules. Acta Crystallogr. C 46, 2442–2445.
Miki, K., Masui, A., Kasai, N., Miyata, M., Shibakami, M., Takemoto, K., 1988. New channel type inclusion compound of steroidal bile acid. Structure of 1:1 complex between cholic acid and acetophenone. J. Am. Chem. Soc. 110, 6594–6596.
Nakano, K., Sada, K., Kurozumi, Y., Miyata, M., 2001. Importance of packing coefficients of host cavities in the isomerization of open host frameworks: guest-size-dependent isomerization in cholic acid inclusion crystals with monosubstituted benzenes. Chem. Eur. J. 7, 209–220.
Nakano, K., Sada, K., Miyata, M., 1994. Inclusion compounds of cholic acid with various hydrocarbons and the crystal structure of a 1:1 complex of cholic acid and benzene. Chem. Lett. 23, 137–140.
Nakano, K., Sada, K., Nakagawa, K., Aburaya, K., Yoswathananont, N., Tohnai, N., Miyata, M., 2005. Organic intercalation material: reversible change in interlayer distances by guest release and insertion in sandwich-type inclusion crystals of cholic acid. Chem. Eur. J. 11, 1725–1733.
Oguchi, T., Kazama, K., Fukami, T., Yonemochi, E., Yamamoto, K., 2003. Specific complexation of ursodeoxycholic acid with guest compounds induced by co-grinding. II. Effect of grinding temperature on the mechanochemical complexation. Bull. Chem. Soc. Jpn. 76, 515–521.
Oguchi, T., Kazama, K., Yonemochi, E., Churimaworapan, S., Choi, W.-S., Limmatvapirat, S., Yamamoto, K., 2000. Specific complexation of ursodeoxycholic acid with guest compounds induced by co-grinding. Phys. Chem. Chem. Phys. 2, 2815–2820.
Oguchi, T., Limmatvapirat, S., Takahashi, C., Sungthongjeen, S., Choi, W.S., Yonemochi, E., Yamamoto, K., 1998. Effect of guest species on inclusion compound formation of deoxycholic acid by co-grinding. Bull. Chem. Soc. Jpn. 71, 1573–1579.
Oguchi, T., Tozuka, Y., Hanawa, T., Mizutani, M., Sasaki, N., Limmatvapirat, S., Yamamoto, K., 2002. Elucidation of solid-state complexation in ground mixtures of cholic acid and guest compounds. Chem. Pharm. Bull. 50, 887–891.
Sada, K., Sugahara, M., Kato, K., Miyata, M., 2001. Controlled expansion of a molecular cavity in a steroid host compound. J. Am. Chem. Soc. 123, 4386–4392.
Vogt, F.G., Clawson, J.S., Strohmeier, M., Edwards, A.J., Pham, T.N., Watson, S.A., 2009. Solid-state NMR analysis of organic cocrystals and complexes. Cryst. Growth Des. 9, 921–937.
Waissbluth, O.L., Morales, M.C., Bohne, C., 2006. Influence of planarity and size on guest binding with sodium cholate aggregates. Photochem. Photobiol. 82, 1030–1038.
Yihwa, C., Quina, F.H., Bohne, C., 2004. Modulation with acetonitrile of the dynamics of guest binding to the two distinct binding sites of cholate aggregates. Langmuir 20, 9983–9991.